

Supporting information

**Beneficial effects of cesium acetate in the sequential deposition
method for perovskite solar cells**

*Byeong Jo Kim¹, Gerrit Boschloo^{*1}*

¹ Department of Chemistry-Ångström Laboratory, Physical Chemistry, Uppsala University, Box 523, SE 751 20 Uppsala,
Sweden

** correspondence: gerrit.boschloo@kemi.uu.se (G. Boschloo)*

Supplementary Tables

Table S1. The photovoltaic parameters of PSCs obtained CsAc-0, -3, -5, and -9 in Fig. S2. All parameters are derived from the current density-voltage curve of the forward scan ($V \leq 0$ to $V \geq V_{oc}$) and the reverse scan ($V \geq V_{oc}$ to $V \leq 0$). The Hysteresis index was calculated by $[\text{PCE of reverse scan} - \text{PCE of forward scan}]/[\text{PCE of reverse scan}]$.

	Scan direction	J_{sc} ($\text{mA}\cdot\text{cm}^{-3}$)	V_{oc} (V)	FF	PCE (%)	Hysteresis index
CsAc-0	Forward	24.36	1.04	0.29	7.35	0.56
	Reverse	25.26	1.08	0.61	16.64	
CsAc-3	Forward	25.68	1.09	0.6	16.79	0.06
	Reverse	25.01	1.08	0.66	17.83	
CsAc-5	Forward	24.66	1.04	0.51	13.08	0.28
	Reverse	25	1.08	0.67	18.09	
CsAc-7	Forward	23.86	1.04	0.51	12.66	0.27
	Reverse	24.03	1.08	0.67	17.39	
CsAc-9	Forward	25.19	1.05	0.56	14.81	0.17
	Reverse	25.42	1.06	0.66	17.78	

Table S2. The photovoltaic parameters of champion devices of CsAc-0 and CsAc-1 in Fig. 1d. . All parameters are derived from the current density-voltage curve of the forward scan ($V \leq 0$ to $V \geq V_{oc}$) and the reverse scan ($V \geq V_{oc}$ to $V \leq 0$). The Hysteresis index was calculated by $[\text{PCE of reverse scan} - \text{PCE of forward scan}]/[\text{PCE of reverse scan}]$.

	Scan direction	J_{sc} ($\text{mA}\cdot\text{cm}^{-3}$)	V_{oc} (V)	FF	PCE (%)	Hysteresis index
CsAc-0	Forward	25.26	1.065	0.703	18.91	0.13
	Reverse	25.20	1.090	0.795	21.84	
CsAc-1	Forward	25.42	1.073	0.745	20.32	0.08
	Reverse	25.45	1.094	0.797	22.19	

Table S3. The photovoltaic parameters of maximum power point tracking test of **a** CsAc-0 and **b** CsAc-1. The number in parentheses of Day 2 indicates relative normalized PCE based on 1st measurement of Day1.

a CsAc-0

CsAc-0	Time (min)	J_{sc} (mA·cm ⁻³)	V_{oc} (V)	FF	PCE (%)	Normalized PCE
Day 1	0	25.77	1.13	77.97	22.71	1.000
	10	25.82	1.08	77.67	21.64	0.953
	20	25.59	1.07	76.93	21.01	0.925
	30	25.54	1.06	74.99	20.28	0.893
	40	24.74	1.05	74.70	19.46	0.857
	50	24.43	1.05	73.24	18.73	0.825
	60	24.38	1.05	72.00	18.35	0.808
	70	24.62	1.04	70.62	18.17	0.800
Keep in dark for 24 hours						
Day 2	0	25.10	1.10	78.38	21.56	1.000 (0.949)
	10	24.87	1.04	77.17	19.97	0.926 (0.879)
	20	24.62	1.02	73.70	18.50	0.858 (0.815)

b CsAc-1

CsAc-1	Time (min)	J_{sc} (mA·cm ⁻³)	V_{oc} (V)	FF	PCE (%)	Normalized PCE
Day 1	0	25.51	1.12	78.71	22.48	1.0000
	10	25.50	1.11	78.67	22.24	0.9894
	20	25.51	1.10	78.29	21.88	0.974
	30	25.58	1.09	78.11	21.87	0.973
	40	25.56	1.09	77.52	21.60	0.961
	50	25.49	1.09	77.27	21.42	0.953
	60	25.48	1.08	77.42	21.39	0.951
	70	25.47	1.08	76.83	21.15	0.941
Keep in dark for 24 hours						
Day 2	0	25.88	1.13	76.07	22.15	1.000 (0.985)
	10	26.24	1.09	76.67	21.83	0.986 (0.971)
	20	26.05	1.07	76.23	21.29	0.961 (0.947)

Table S4. The fitted XPS parameters of Pb, I, Cs as deposited PbI_2 -0, -1, and -2 sample.

		PbI_2-0		PbI_2-1		PbI_2-2	
Pb		Pb $4f_{7/2}$	Pb $4f_{7/2}$	Pb $4f_{7/2}$	Pb $4f_{7/2}$	Pb $4f_{7/2}$	Pb $4f_{7/2}$
	Peak energy (eV)	138.43	136.67	138.38	136.64	138.27	136.49
	FWHM (eV)	0.79	0.98	0.76	0.87	0.80	0.87
	Area (%)	95.03	4.97	93.53	6.47	93.92	6.08
I		I $3d_{5/2}$		I $3d_{5/2}$		I $3d_{5/2}$	
	Peak energy (eV)	619.18		619.18		618.97	
	FWHM (eV)	0.90		0.88		0.90	
	Area (%)	100		100		100	
Cs		Cs $3d_{5/2}$		Cs $3d_{5/2}$		Cs $3d_{5/2}$	
	Peak energy (eV)			724.49		724.37	
	FWHM (eV)			1.27		1.25	
	Area (%)			100		100	

Table S5. The extracted parameter from the XRD data in Fig.3e for Williamson-Hall Plot. The Williamson-Hall Plot is drawn in Fig. S11 with $4\sin\theta$ along the x-axis and $(FWHM \times \cos\theta)$ along the y-axis.

a. CsAc-0

No.	(hkl)	2θ (Degree)	FWHM in degree	$FWHM \times \cos\theta$	$4\sin\theta$
1	(001)	13.96449	0.35316	0.006118	0.486247
2	(111)	24.37637	0.34959	0.005964	0.844493
3	(002)	28.22068	0.34096	0.005771	0.97516
4	(012)	31.63347	0.38193	0.006414	1.090245
5	(022)	40.37374	0.3953	0.006475	1.380332
6	(003)	42.9328	0.38973	0.00633	1.463822

b. CsAc-1

No.	(hkl)	2θ (Degree)	FWHM in degree	$FWHM \times \cos\theta$	$4\sin\theta$
1	(001)	13.96857	0.35359	0.006126	0.486388
2	(111)	24.5062	0.34372	0.005862	0.848922
3	(002)	28.40235	0.3407	0.005765	0.981309
4	(012)	31.67897	0.37949	0.006372	1.091773
5	(022)	40.38507	0.39054	0.006397	1.380704
6	(003)	42.96297	0.38519	0.006256	1.464802

c. CsAc-3

No.	(hkl)	2θ (Degree)	FWHM in degree	$FWHM \times \cos\theta$	$4\sin\theta$
1	(001)	13.97	0.35849	0.00621	0.486354
2	(111)	24.58	0.34631	0.005906	0.851415
3	(002)	28.44	0.33995	0.005751	0.982458
4	(012)	31.67	0.38078	0.006394	1.09147
5	(022)	40.39	0.38869	0.006367	1.380752
6	(003)	42.95	0.39164	0.006361	1.464273

Table S6. TRPL amplitudes and lifetimes of the CsAc-0, and -1 samples. A_i and τ_i are the amplitude ratio and lifetime of each component, respectively. The intensity weighted average lifetime was calculated by $\tau_{avg} = \sum A_i \tau_i^2 / \sum A_i \tau_i$

Samples	A_1 (%)	τ_1 (ns)	A_2 (%)	τ_2 (ns)
Glass/CsAc-0	6.1	45.99	93.9	1020.9
Glass/CsAc-1	4.2	16.40	95.8	1140.12

Table S7. The extracted absorption onset of CsAc-0, and -1 samples during thermal stability test.

Absorption onset [nm]	20 °C (1 minute)	120 °C (7 minute)	120 °C (500 minute)	280 °C (508 minutes)	Initial – final band onset
CsAc-0	805.9	783.4	781.8	797.5	8.4 (blue shift)
CsAc-1	808.4	782.8	786.2	806.2	2.2 (blue shift)

Supplementary Figures

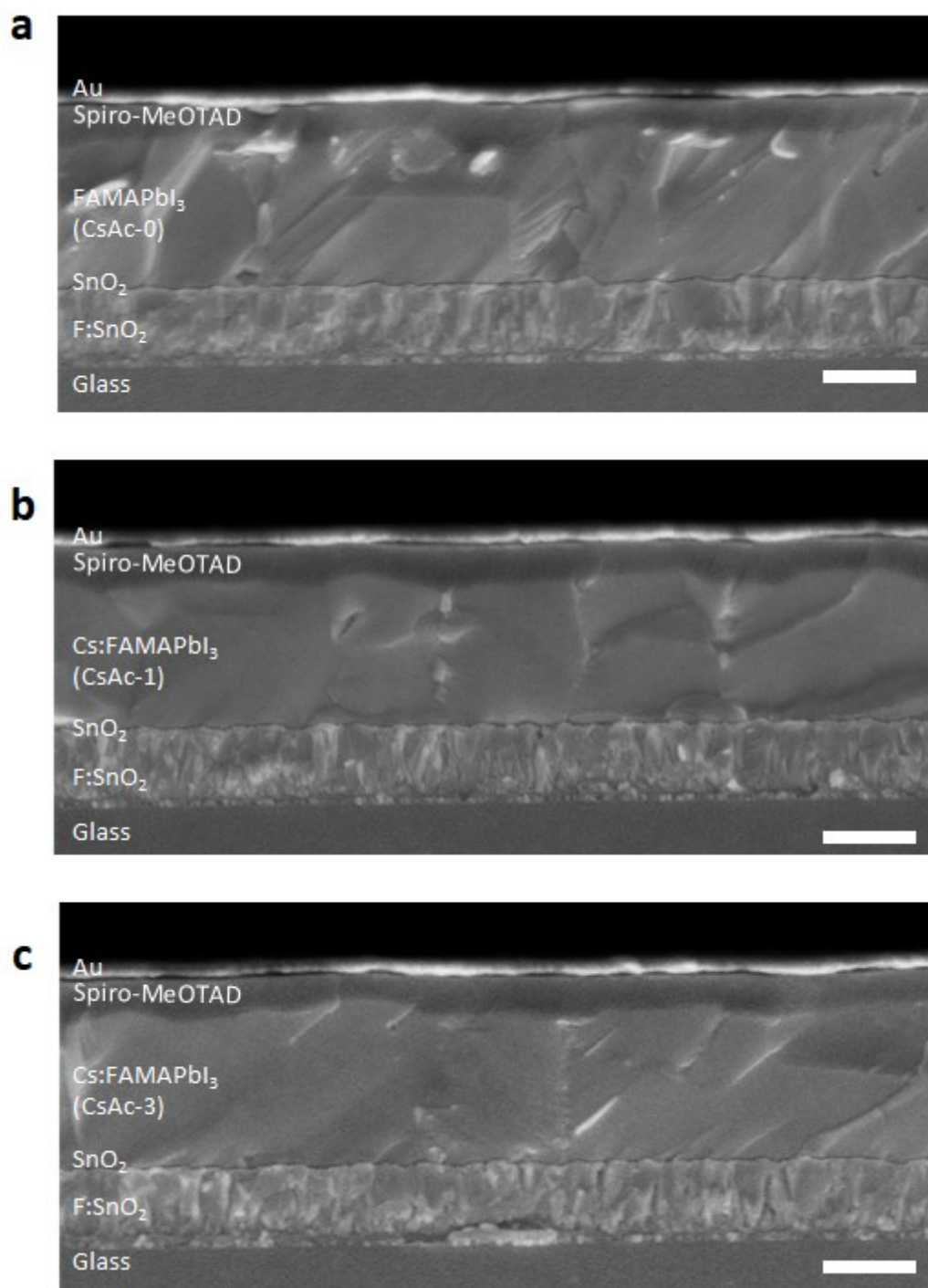


Fig. S1. The cross-sectional SEM images of PSCs obtained (a) CsAc-0, (b) CsAc-1, and (c) CsAc-3 perovskite layer. The scale bar is 500 nm.

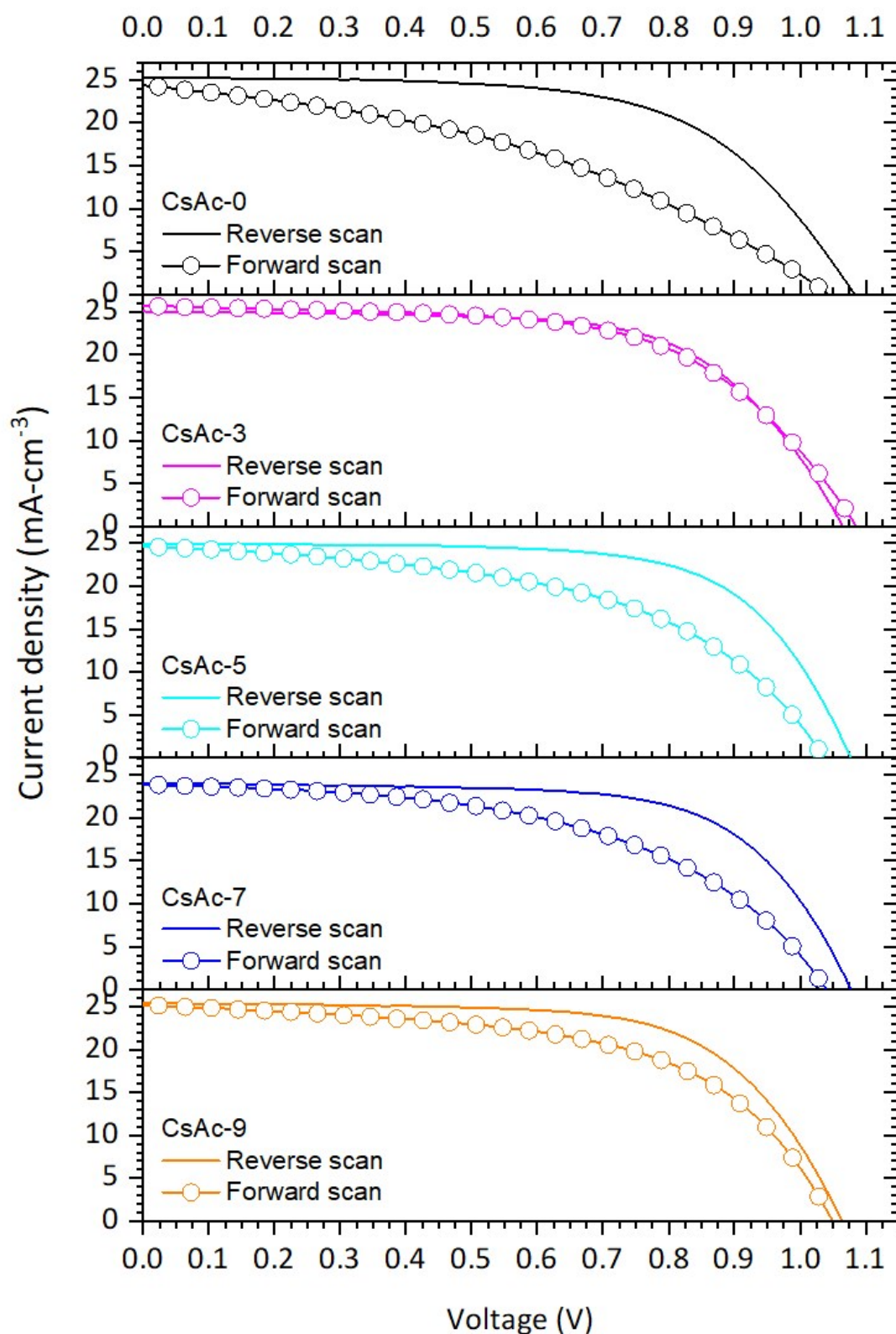


Fig. S2. J-V curves of PSCs obtained CsAc-0, -3, -5, and -9. The forward scan applied voltage from negative to positive ($V \leq 0$ to $V \geq V_{oc}$) and the reverse scan applied reversed direction ($V \geq V_{oc}$ to $V \leq 0$).

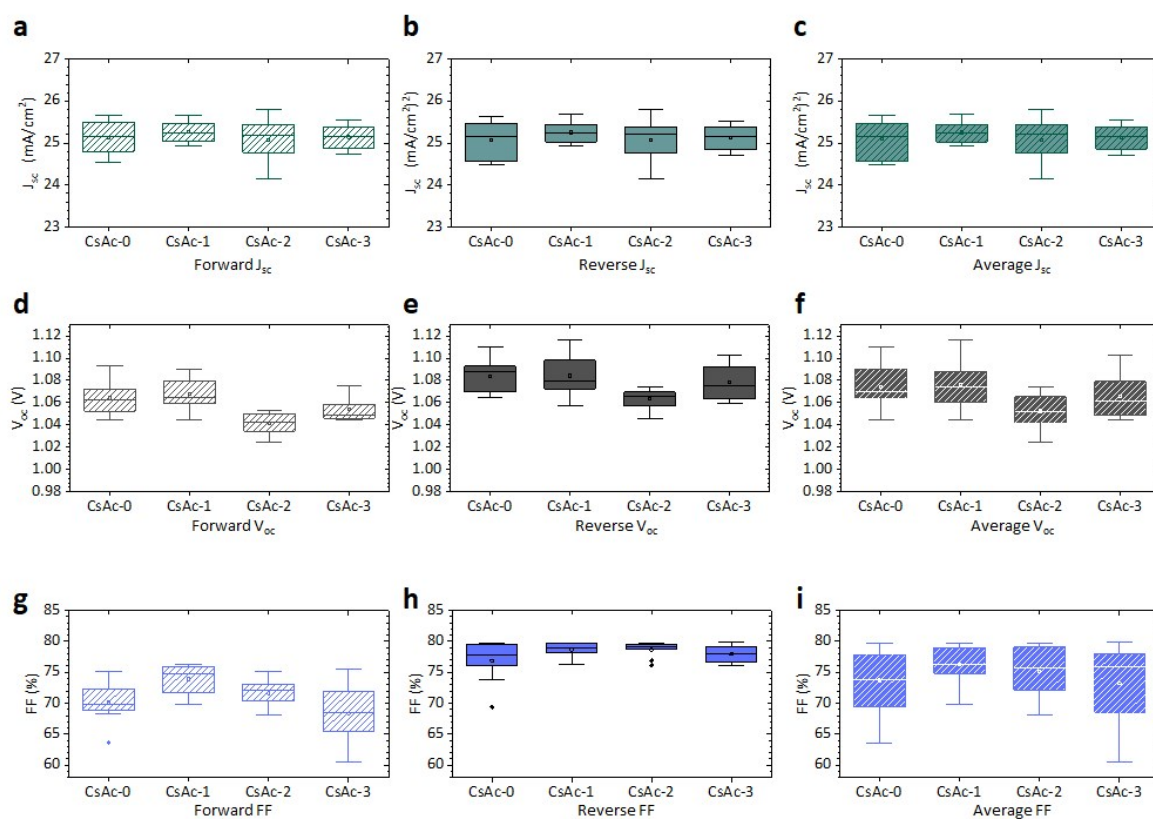


Fig. S3. The statistics box chart of (a-c) J_{sc} , (d-f) V_{oc} , and (g-i) FF extracted from the J - V curves of CsAc-0, -1, -2 and -3. The boxes show the standard deviations, $n=16$; the whiskers represent the 10/90 percentiles; the small squares denote the mean; the two horizontal bars denote the 99% and 1% values.

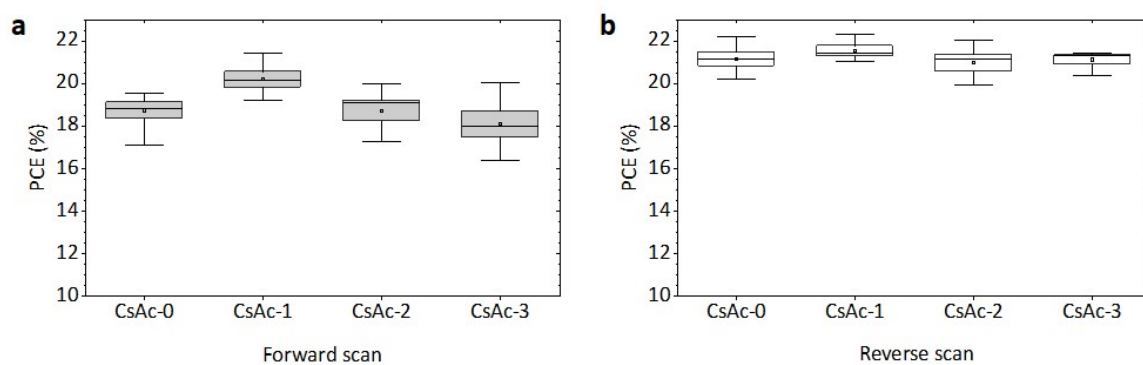


Fig. S4. The statistics of PCE obtained CsAc-0, -1, -2, and -3 PSCs as scan direction. (a) Forward scan, (b) Reverse scan direction. The boxes show the standard deviations, $n= 16$; the whiskers represent the 10/90 percentiles; the small squares denote the mean; the two horizontal bars denote the 99% and 1% values.

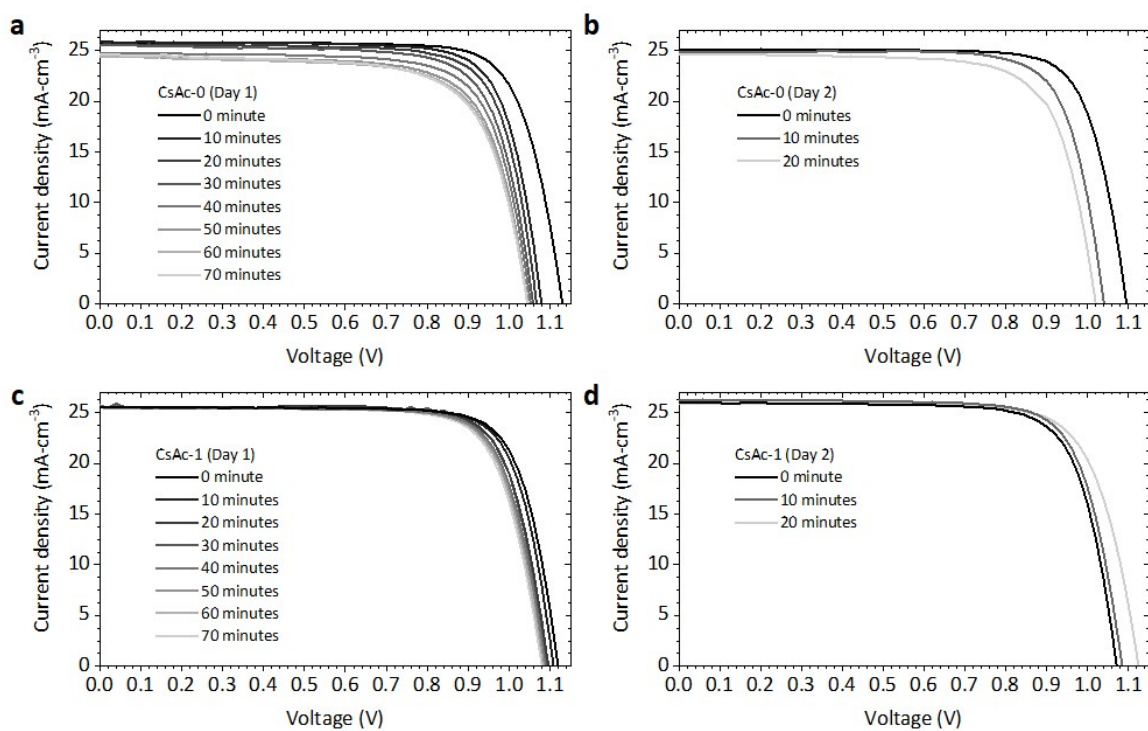


Fig. S5. The J-V curves of (a and b) CsAc-0 and (c and d) CsAc-2 recorded every 10 minutes during maximum power point tracking of CsAc-0 and CsAc-1 solar cells under 1.5 AM simulated sunlight in ambient air corresponding to Fig 1f.

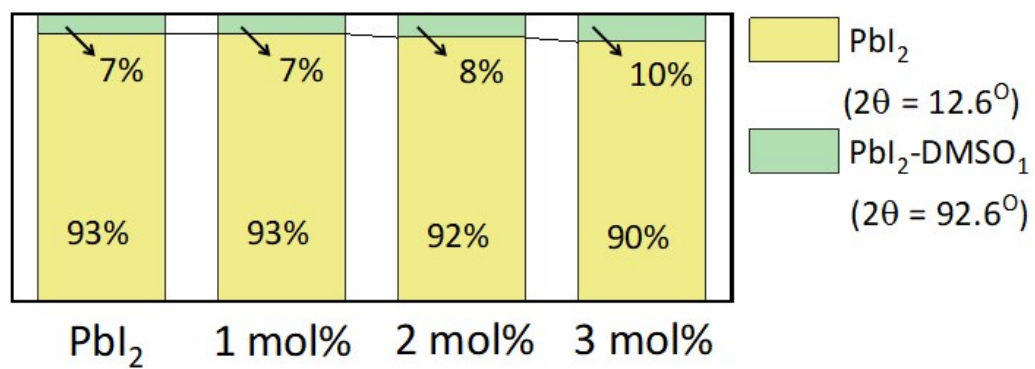


Fig. S6. Relative XRD peak intensity of Pbl₂ and Pbl₂-DMSO, extracted by XRD data in Fig. 2e.

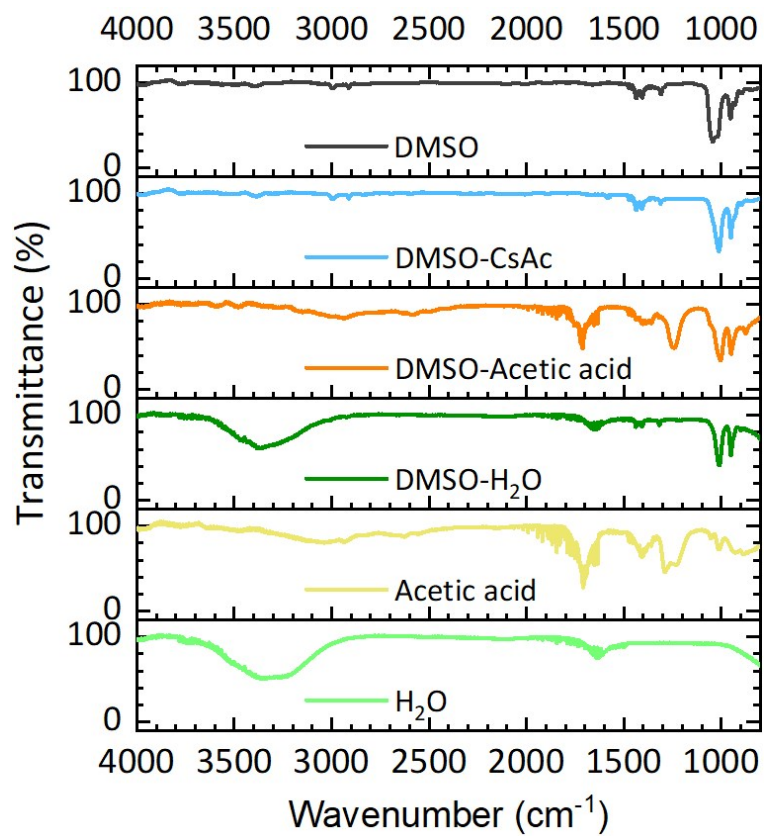


Fig. S7. The full range of FTIR results of DMSO, DMSO-CaAc, DMSO-acetic acid, DMSO-H₂O, acetic acid, and H₂O.

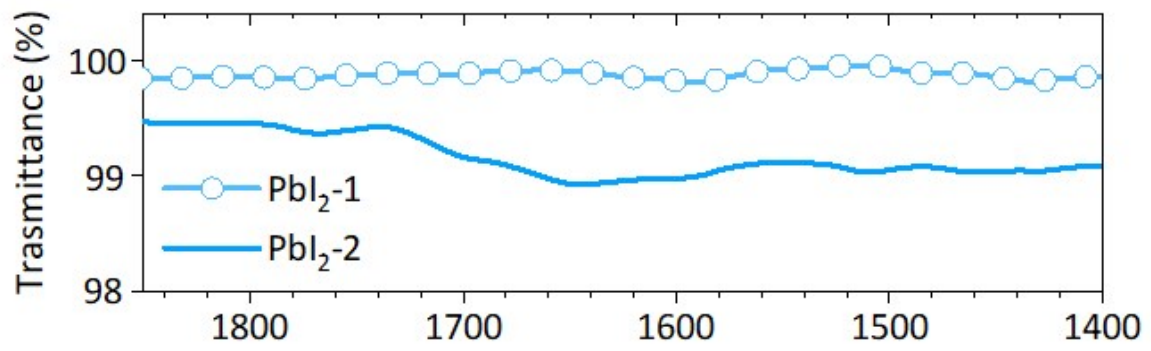


Fig. S8. The FTIR spectra of Pbl₂-1, and Pbl₂-2 films.

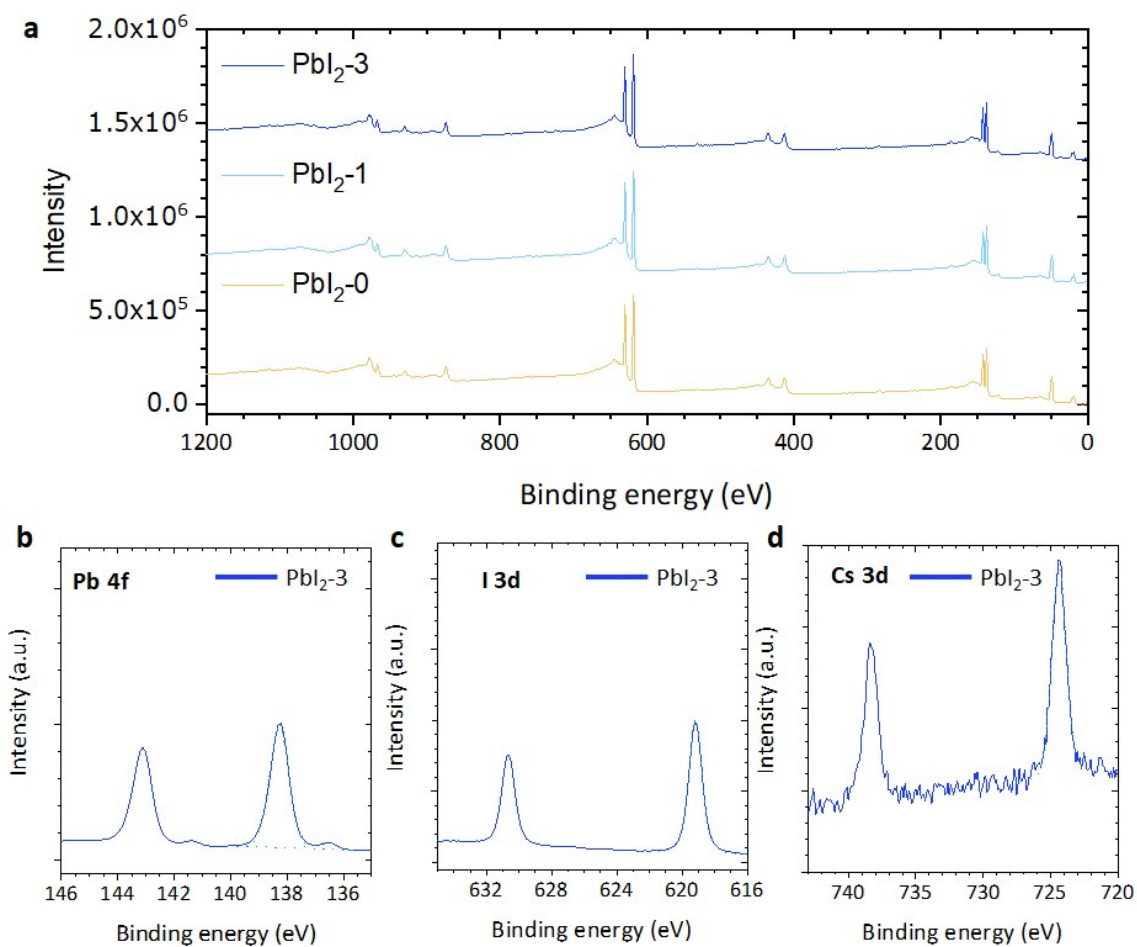


Fig. S9. (a) the full range of XPS measurement data of $\text{Pbl}_2\text{-0}$, -1 and -3 samples. (b) Pb 4f, (c) I 3d, (d) Cs 3d xps spectra of $\text{Pbl}_2\text{-3}$ sample.

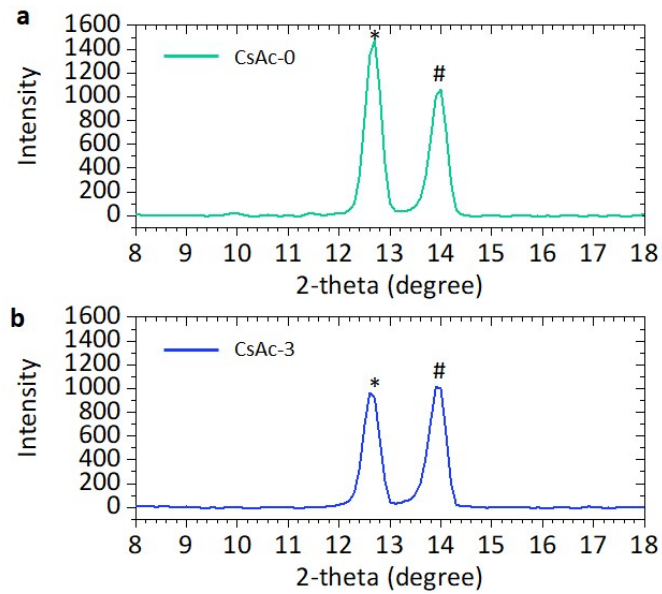


Fig. S10. The grazing incident XRD analysis using incident beam of 1° for (a) CsAc-0 and (b) CsAc-3. * and # indicated PbI_2 at 12.6° and $\alpha\text{-FAPbI}_3$ at 14.0° , respectively.

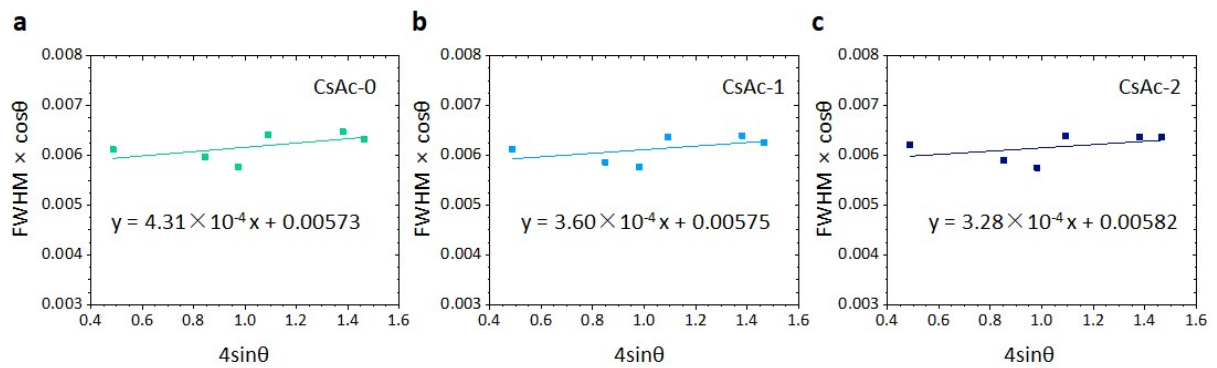


Fig. S11. Williamson-Hall plot with different concentrations of CsAc. Each data points extracted by XRD data in Fig. 3e, and it summarized in Table S5. the relative lattice strain and size component calculated from slope and intercept of linear fitted line.

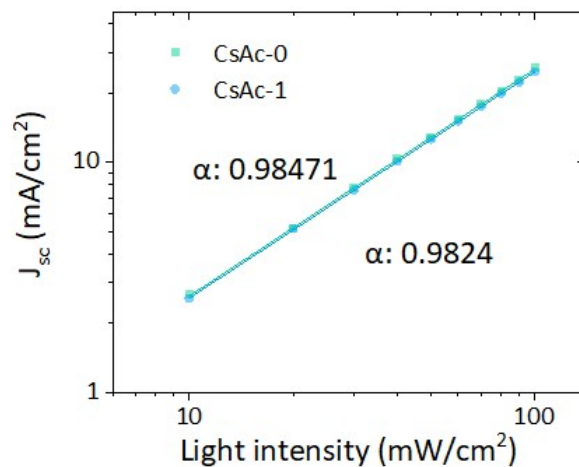


Fig. S12. J_{sc} of CsAc-0, and CsAc-1 PSCs as a function of light intensity, the solid lines denote linear fits to the experimental data.

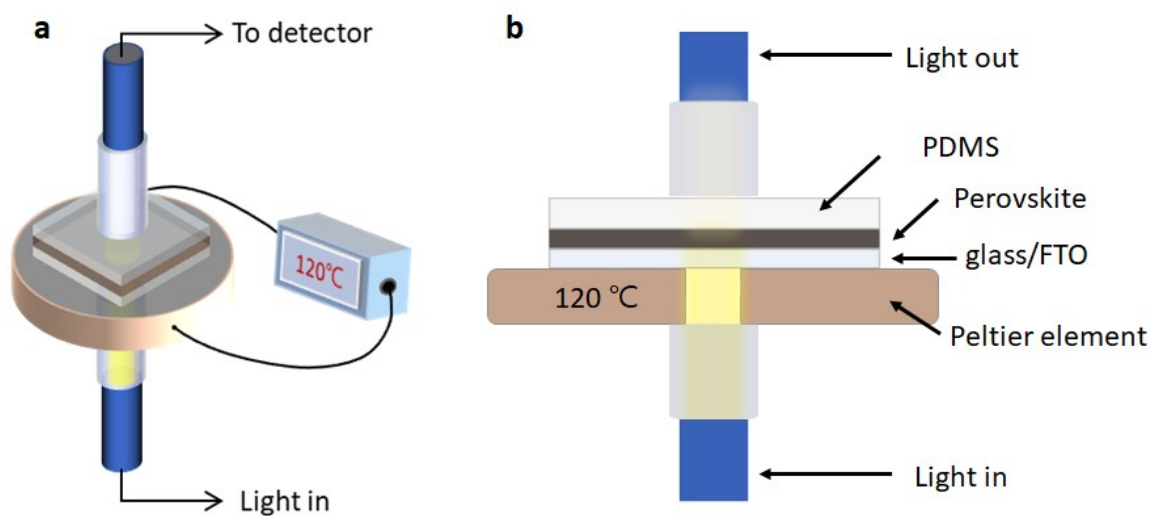


Fig. S13. (a) Schematic image of temperature controlled in-situ UV-Vis spectroscopy for thermal stability. (b) Detailed schematic of the cross-sectional view of heating part.

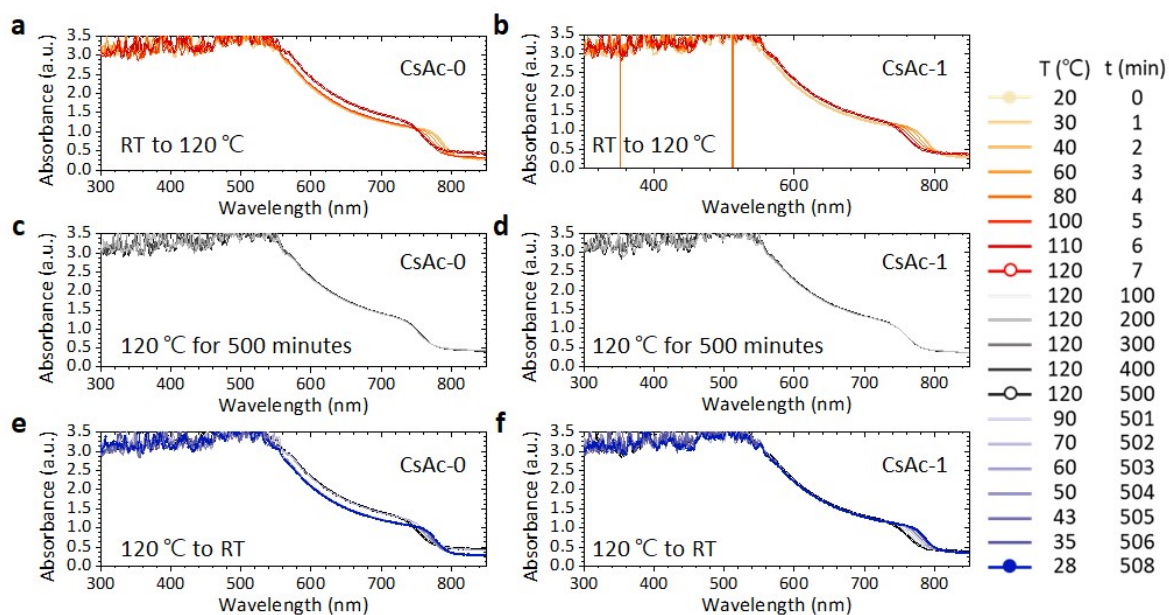


Fig. S14. the full range of absorbance spectrum of (a, c, and e) CsAc-0 and (b, d, and f) CsAc-1 using temperature controllable in-situ the UV-Vis spectroscopy. (a and b) Upper spectra (RT to 120 °C), temperature increased 20 °C per minutes. (c and d) And then temperature keeps 120 °C until 500 minutes. (e and f) After 500 minutes, the temperature was spontaneously cool down to RT and the temperature was recorded every 1 minute. UV-vis spectra were recorded every 1 min for 510 minutes.

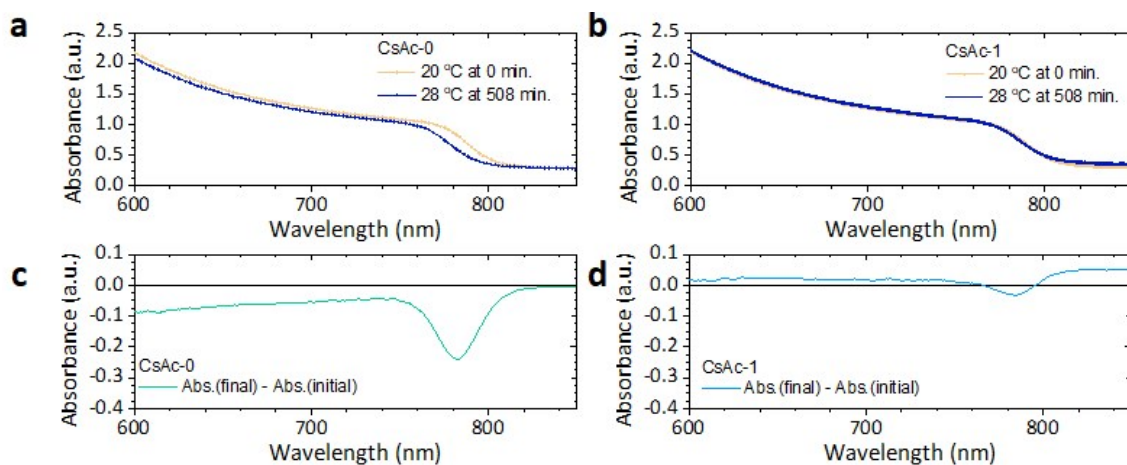


Fig. S15. The initial and final absorbance spectrum of (a) CsAc-0 and (b) CsAc-1 corresponding to Fig. 4 and Fig. S13. The difference in absorbance between the final measurement and the initial measurement represented in (c) CsAc-0 and (d) CsAc-1, respectively. A positive value in (c) and (d) means the increased absorbance spectrum after thermal stress test. A negative value is opposite.